Journal of Robotics and Control (JRC)
Volume 3, Issue 5, September 2022
ISSN: 2715-5072, DOI: 10.18196/jrc.v3i5.15944

Electric Wheelchair Hybrid Operating System Coordinated with Working Range of a Robotic Arm

Laijun Yang [1, *], Nan Guo [2], Ryota Sakamoto [3], Norihiko Kato [4], Ken'ichi Yano [5]
[1, 2, 4,5] Graduate School of Engineering, Mie University, Mie, Japan
[3] Mie University Hospital, Mie, Japan
Email: [1] ljyang@robot.mach.mie-u.ac.jp, [2] kakunan@robot.mach.mie-u.ac.jp, [3] sakamoto@robot.mach.mie-u.ac.jp,
[4] nori@robot.mach.mie-u.ac.jp, [5] yanolab@robot.mach.mie-u.ac.jp
*Corresponding Author

***Abstract*— Electric wheelchair-mounted robotic arms can help patients with disabilities to perform their activities in daily living (ADL). However, to stop the wheelchairs in an appropriate position for the robotic arm grasping task is not easy for the patients with upper limb dysfunction. In order to reduce the individual's burden in operating wheelchair in narrow spaces and to ensure that the wheelchair always stops within the working range of a robotic arm. This study presents an operating system for an electric wheelchair that can automatically drive itself to within the working range of a robotic arm by capturing the position of an AR marker via a chair-mounted camera. Meanwhile, in order to correct the accumulated moving error of electric wheelchair, the system also include the error prediction and correction model to correct the wheelchair's moving error without modelling the electric wheelchair. Finally, comparing the wheelchair's moving track demonstrates the effectiveness of the model for predicting and correcting movement errors. Simulating the robotic arm across serval courses demonstrates that the proposed system can cause the wheelchair to halt in the proper position to finish the grasping work. To compared with the previous research, we correct the moving error modifying the trajectory of electric wheelchair which keeps the AR marker in the visual field during the hole running process, which fundamentally solved this problem.**

Keywords*— Electric wheelchair; Self-driving; Robotic arm; GUI (graphical user interface); Error correction.

I. INTRODUCTION

There are currently many handicapped people in Japan who face limitations in their daily lives because of physical disabilities resulting from accidents or illnesses. According to a survey conducted by the Ministry of Health, Labor, and Welfare, in 2018 there were 4.36 million people with disabilities in Japan [1]. This represents a 19% increase in 5 years when compared to 3.66 million in 2013 [2]. It is estimated that 1.93 million people, or approximately 44% of the handicapped, are physically disabled. Spinal cord injury, cerebrovascular disease, cerebral palsy, muscular dystrophy, and ALS are examples of diseases that cause physical handicaps. Wheelchairs are an essential way of transportation for people with these diseases. In recent years, electric wheelchair-mounted robotic arms are being developed to help patients with disabilities to perform their daily activities [3-7]. Such activities involve reaching for everyday objects such as food or drink, books, and so on. The commonly used operating interfaces for electric wheelchair-mounted robotic arms are joysticks or keypads [8]. However, under different scenarios, some patients with upper limb disabilities such as finger contracture cannot operate such interfaces smoothly. To solve this problem, some new operating interfaces were developed. Interfaces that change the input device to match the symptoms without requiring the mode switching operation arm to be developed, such as 3D mouse and gesture-based interface [9-11]. Also, Interfaces that operates wheelchair-mounted robotic arms by recognizing voice commands are also being proposed [12-15]. Meanwhile, the bioelectric signals, such as electroencephalograms (EEGs), electromyograms (EMGs), and electrooculograms (EOGs) were also utilized to understand a user's intention to operate electric wheelchairs [16-19].

Utilizing these interfaces makes the operation of electric wheelchair-mounted robotic arms accessible to patients with upper limb dysfunction [20-22]. However, let us consider an ADL scenario, having an electric wheelchair, with an attached robotic arm that aims to pick up objects from the floor or desk. This task can be separated into two main parts: first, the user must move the wheelchair to an appropriate position near the object. Second, the robotic arm must be moved such that it grasps the object and brings it to the user. In this scenario, the posture of the robotic arms end effector is different according to the different grasping tasks. It is important to move the wheelchair to an appropriate position to ensure the target object is easy to reach, which is difficult to achieve in manual operation. Meanwhile, fine adjustment of the electric wheelchair is not easy when the robotic arm is outstretched and presents a severe physical burden on patients with quadriplegia or other conditions [23], [24]. When operating the electric wheelchair with the manual interfaces, it is easy to reach the target position in a wide space. However, as a non-holonomic system, electric wheelchairs cannot move laterally, that means even the fine adjustment of position needs to repeatedly tilt the joystick by a small amount [25].

On the other hand, when the caster in opposite direction with the movement of the electric wheelchair, the moving direction of wheelchair will be different with the operator's intention. Therefore, even for the healthy operator, it is difficult to fine-adjust the position of wheelchair near the target object. Especially for the patients with upper limb dysfunction, to accomplishing such operation requires the increase of operation frequency and more physical burden [26]. To counter these issues, self-driving electric

wheelchairs have become a meaningful concept in recent years. When an electric wheelchair is near a target object, self-driving capability can not only ensure to stop the wheelchair in an appropriate position for the robotic arm but also reduce the physical tension that the operator experiences.

In recent years, the self-driving technology has been a great development [27-30]. Recently, such technology was also utilized in electric wheelchairs. 2D/3D mapping-based system is one of them [31-34]. In such a system, a 2D/3D map is built from the information acquired by wheelchair-mounted 2D/3D LiDAR [35]. The self-localization can be estimated by the normal distribution transform [36]. Then, the route of self-driving can be generated by the waypoints acquired by the traveled routes [37]. But these mapping systems were usually built by path tracking of manual operation the first time a route is run [38]. GPS-based self-driving systems were also being proposed [39-42]. These systems performed well in an outdoor environment, but GPS is not sufficient in tight indoor environments. Recently, Virtual Reality was also used in self-driving systems [43-47]. These systems using a head-mounted display (HMD) device to build real-time 3D mapping, and to avoid the obstacles by utilizing the existing software library [48]. But always wearing an HMD device is a physical burden to the operator in practical use [49]. On the other hand, as an easier feasibility way, position estimation system based on AR marker recognition has been widely used recently. This technology was also applied in self-driving in electric wheelchair [50-53]. However, because the position of the sensors is fixed, such interfaces have issues with losing sight of the AR tag while running. To solve this problem, position prediction system based on wheelchair modelling is also proposed. However, the simplified wheelchair modeling is insufficient for practical use, resulting in position prediction failure [54].

Although several self-driving interfaces were proposed, it is difficult to achieve full self-driving in a real, complex environment [55]. Meanwhile, the more sensors attached means the higher cost of the system.

Stopping the electric wheelchair in an appropriate position becomes an important question in using a wheelchair-mounted robotic arm. However, the manual interfaces have the problem in fine adjustment. On the other hand, the fully autonomous systems have some limits in practical use. In this study, we focus on the operation of an electric wheelchair in wheelchair-mounted robotic arm system. We proposed a hybrid operating system for an electric wheelchair that coordinated with the working range of a robotic arm that includes both a manual operating mode and a self-driving mode. In manual mode, the wheelchair can be operated by using an on-screen joystick for daily movement. In self-driving mode, by using a camera to recognize an AR marker attached to a target object, the wheelchair will drive itself close to the target so that it is within the robotic arm's working range. Meanwhile, in order to solve the problem that the moving direction of wheelchair is different with the expectation, we proposed a moving error prediction and correction model by collecting and analyzing the advance moving data of electric wheelchair which avoid the complicated wheelchair modelling. The proposed system modifies the trajectory of wheelchair which make sure the target AR marker keep in the visual field of camera during running.

The rest of the paper is presented in the following order. Section II discusses the stop condition of wheelchair. The graphic user interface (GUI) proposed in this research is discussed in section III. In section IV, the moving error of electric wheelchair is defined and modeled, Experimental parameters and comparison of the result are given in section V. Finally, conclusions are drawn in section VI.

II. WORKING RANGE OF ROBOTIC ARM

To stop the electric wheelchair once it is within the working range of the robotic arm, in this section, we discuss the stopping condition of the self-driving system. Fig. 1 and Fig. 2 show the structure of the robotic arm and the mounting position on the electric wheelchair. Since we know the relative positions of the camera and the AR marker, the relative positions of the robotic arm and AR marker can be calculated by the coordinate transformation.

Usually, the different grasping tasks require the different posture of the robotic arms end effector, so that the appropriate stop position of the wheelchair depends on the different operations of robotic arm. In our former research, we proposed a robotic arm operating interface which can recognize the position of the target object by a camera mounted on the end effector and choose the specific posture to grasp the object automatically [56]. Since this work is focused on wheelchair movement, here we simply set the stopping condition of the electric wheelchair as the maximum working range of the robotic arm.

Fig. 1. Mounting position of camera on electric wheelchair

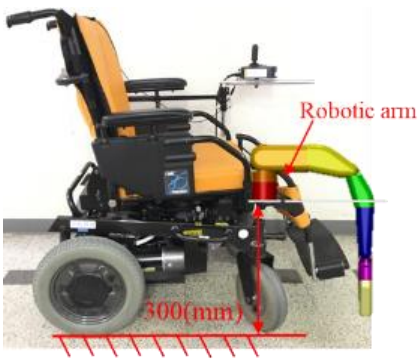

Fig. 2. Mounting position of robotic arm on wheelchair

Fig. 3 shows the working range of a robotic arm named "Udero" [57]. The working range can be divided into an upper part and a lower part according to the structure of the robotic arm. To ensure that the operator does not collide with the arm during operation, and to ensure that the operator is easily aware of the surrounding operating environment, we set the robotic arm's working range in the horizontal plane as the condition of $\varphi_{\min} \le \varphi \le \varphi_{\max}$ where $\varphi_{min} = -30(\text{deg})$ and $\varphi_{max} = 90(\text{deg})$ as shown as Fig. 4. Therefore, according to the arm's working range in the horizontal plane, when the relative height of the arm and the AR marker $h_l \ge 0$ (which means the marker is higher than the root of the arm), the self-driving stop condition can be calculated by (1), where $P_m(x_m, y_m, z_m)$ represents the relative position of the AR marker to the base of the robotic arm as the origin. R represents the length between the second and the seventh joints of the robotic arm.

$$\begin{cases} \sqrt{x_m^2 + y_m^2 + z_m^2} < R \\ \varphi_{\min} < \text{sgn}(y_m)\cos^{-1}\dfrac{x_m}{\sqrt{x_m^2 + y_m^2}} < \varphi_{\max} \end{cases} \quad (1)$$

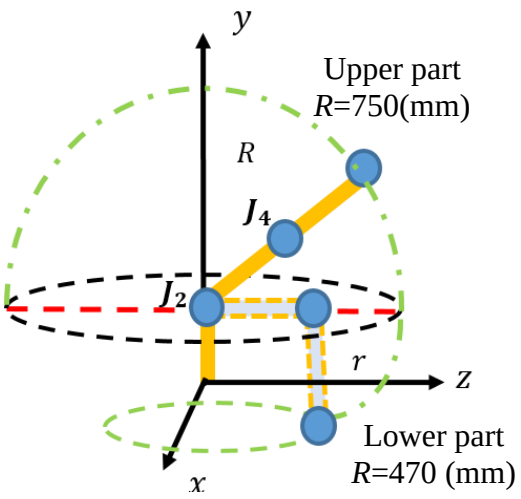

Fig. 3. Working range of the robotic arm

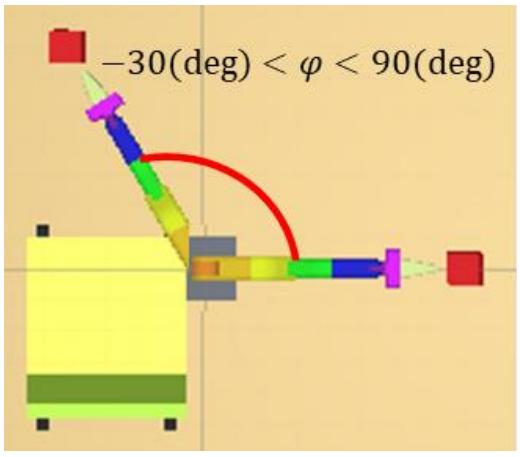

Fig. 4. Specified working range in the horizontal plane

On the other hand, when $h_l < 0$, the self-driving stop condition can be calculated by (2),

$$\begin{cases} \sqrt{(x_m - l\cos\varphi)^2 + y_m^2 + (z_m - l\sin\varphi)^2} < r \\ \varphi_{\min} < \text{sgn}(y_m)\cos^{-1}\dfrac{x_m}{\sqrt{x_m^2 + y_m^2}} < \varphi_{\max} \end{cases} \quad (2)$$

III. GRAPHIC USER INTERFACE

In this research, we propose a hybrid operating system to give an electric wheelchair both a manual operating mode and a self-driving mode. The graphical user interface (GUI) used in this study was developed with the Unity Technologies software library.

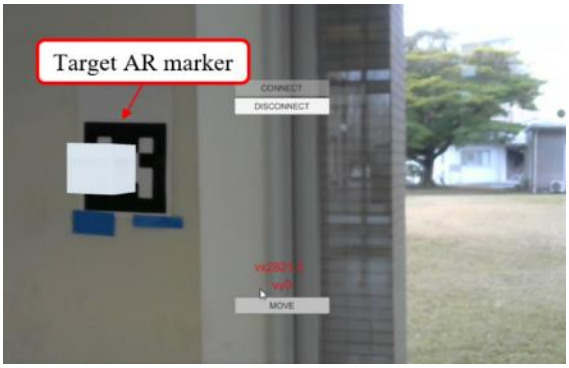

Fig. 5. Proposed GUI

The proposed GUI incorporates both a manual mode and a self-driving mode. The manual interface is based on our previous study [58] [59], features an on-screen joystick suitable for patients with cervical spinal cord injury. The wheelchair can be operated manually by the operator dragging this on-screen joystick. The background of the GUI is a real-time scene taken by a web camera. The "CONNECT" and "DISCONNECT" buttons at the top of the screen are used to enable the operator to communicate with the wheelchair. After pressing "CONNECT" button, the operator can move the wheelchair close to the target position manually. In manual mode, once the touch operation is detected, the joystick button is displayed on the first touchpoint on the screen. The manipulated variable of the joystick $\boldsymbol{T}$ in both the longitudinal and crosswise directions can then be calculated by the dragging information from the joystick, the information is then sent to the wheelchair.

Fig. 5 shows interface in the self-driving mode, after the wheelchair reaches the vicinity of the target position, the web camera captures the AR marker attached to the target object, and the system switches automatically to self-driving mode. At this time, if the operator presses and holds the "MOVE" button at the bottom of the screen, the electric wheelchair will move toward the target position automatically. In self-driving mode, once the wheelchair-mounted web camera catches the AR marker attached to the target object, the real-time relative position and posture between the marker and the camera are obtained by using ARToolKit software [60]. The control module then calculates the manipulated variable of the joystick $\boldsymbol{T}$ in the longitudinal direction with T_y, and that in

the crosswise directions with T_x according to the relative position information by (3), where $\boldsymbol{P}$ (x, y) represents the relative position between the camera and the AR marker with the latter as the origin. G represents the electric wheelchair's speed gain.

$$\boldsymbol{T} = \begin{bmatrix} T_x \\ T_y \end{bmatrix} = G \begin{bmatrix} x \\ y \end{bmatrix} \quad (3)$$

IV. PREDICTIOPN AND CORRECTION OF MOVING ERROR

A. Moving Error of Electric Wheelchair

To verify the performance of the proposed GUI, we did an operation experiment to running the wheelchair using the proposed GUI in the indoor environment. The task of the experiment is for the operator to use the proposed GUI to move the wheelchair to within the robotic arm's reach to the target position. We put the electric wheelchair in 30 random initial positions as shown as Fig. 6, where the camera can recognize the AR marker. The wheelchair used in this experiment was an EMC-270 made by Imasen Engineering Corporation, as shown in Fig. 2. During the experiment, we noted that as both the distance and the angle formed between the initial and target positions increase, the target AR marker disappear from the camera's visual field, thus preventing the wheelchair from arriving near the target position. We consider that the moving error of electric wheelchair is driven by two factors. The first is the precision of position estimation by AR marker recognition. The second is thought to be a time delay in the electric wheelchair's reception of the control signal, which causes the wheelchair mounted camera to lose the target AR marker while the wheelchair is being moved at a rapid rate of speed.

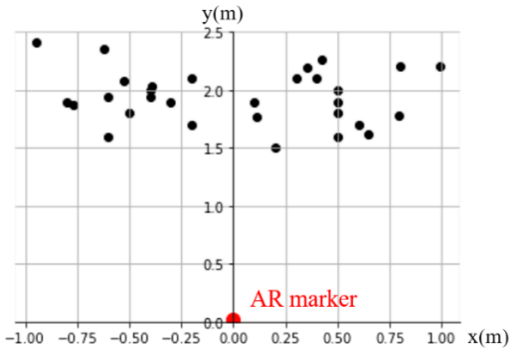

Fig. 6. The experimental task in operation check

In order to clarify the moving error, at first, we define the moving error as shown in Fig. 7. As the figure shows, point $P(x_0, y_0)$ represents the target position, and point $A(x_a, y_a)$ represents the initial position of the wheelchair. θ represents the angle formed between the wheelchair's initial position and the AR marker where the wheelchair faces forward. L represents the distance between initial position A and target position P. dx represents the ideal amount of movement of wheelchair in crosswise direction. At position A, once the camera captures the AR marker, the wheelchair begins to self-drive. We assumed that the marker disappears from the camera's visual field when the wheelchair arrives at position $B(x_b, y_b)$. When the wheelchair gets to B, the manipulated variable of the joystick is T_B, with T_{by} and T_{bx} in crosswise directions respectively. The wheelchair then drives straight and keeps the manipulated variable as T_B until the trajectory intersects the x-axis in position C. Here, we define the distance between position $C(x_c, y_c)$ and target position P as the moving error represented by e, which can be calculated by (4).

$$e = (y_b - y_0)\frac{T_{bx}}{T_{by}} + (x_b - x_0) \quad (4)$$

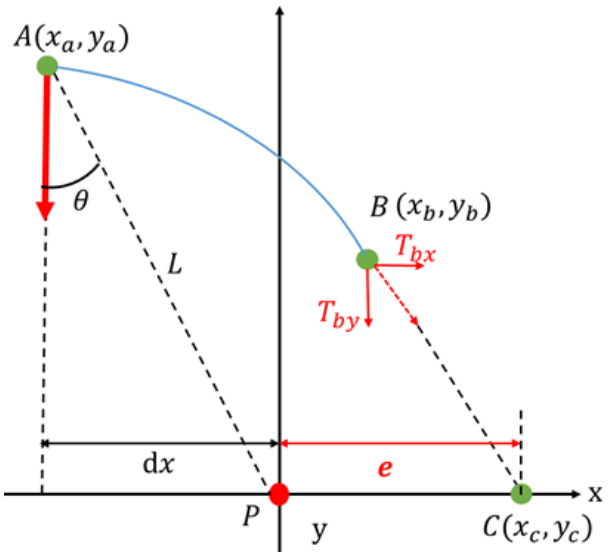

Fig. 7. Definition of moving error

B. Accuracy of Position Estimation by Marker Recognition

Since the accuracy of position estimation by AR marker have a great impact on the movement of electric wheelchair [61] [62], we first verified the recognition accuracy of the AR marker in 14 different positions. The result is shown in Fig. 8.

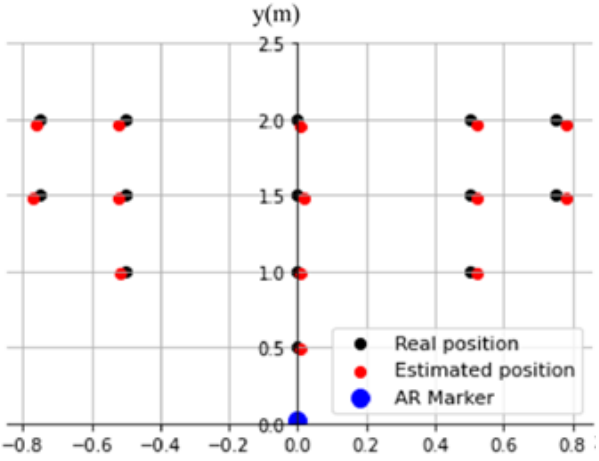

Fig. 8. Result of position estimation

In Fig. 8, the black points represent the real position of a camera mounted on an electric wheelchair, the red points represent the position estimation from AR marker recognition. As the result, we find that as the distance increases, the error of position estimation becomes bigger. However, the average error is 0.03m, which is acceptable to compare with the distance between electric wheelchair and AR marker.

C. Relationship Between Moving Error and initial Position

To clarify the relationship between moving error and initial state of electric wheelchair, we measured each distance L and the angle θ formed between the initial and target positions in the running experiment. We also measured and calculated the error e of each random initial state.

First, we did a single linear regression analysis between θ and e and another between L and e. The results are shown in Fig. 9 and Fig. 10, respectively. Since we thought there is no error when $L = 0$ and $\theta = 0$, the regression line in Fig. 9 and Fig. 10 pass the origin. In Fig. 9, the moving error e is moderately correlated with the initial angle θ. The correlation coefficient equals 0.914. The circled variation was caused by the caster in opposite direction with the movement of electric wheelchair. This can be easily solved by moving the electric wheelchair forward in manual mode. Thus, we treat these values as outliers. On the other hand, in Fig. 10, the correlation between L and e is low with the correlation coefficient as 0.538. However, when the formed angle is about the same, L and e have a high correlation with a correlation coefficient of 0.914. Finally, we use multiple linear regression to build a prediction model of moving error. The result is represented by (5).

$$e \cong 0.244L + 0.024\theta - 0.473 \quad (5)$$

Meanwhile, the coefficient of determination equals 0.874 and the mean squared error equals 0.004, which shows that this prediction model is highly accurate.

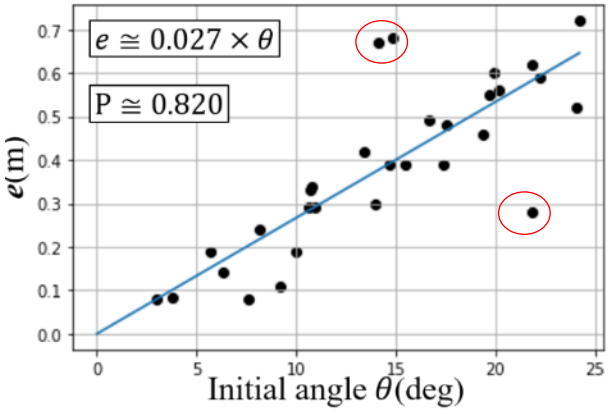

Fig. 9. Relationship between e and initial angle θ

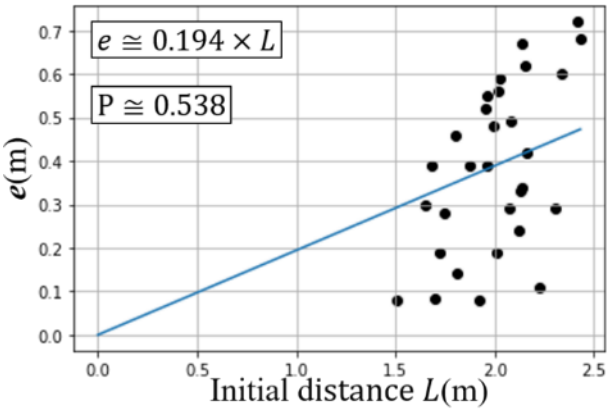

Fig. 10. Relationship between e and distance L

D. Correction of the Manipulated Variable of the Joystick

After building the prediction model of moving error, we calculate the manipulated variable correction coefficient of the joystick according to the predicted moving error e. As Fig. 11 shows, A and P represent the initial and target positions, $\boldsymbol{Q}(x_t, y_t)$ represents the position of the wheelchair in time t, and e_t represents the predicted moving error in time t. Therefore, the manipulated variable correction coefficient K_t can be calculated as (6).

$$K_t = x_t/(x_t + e_t) \quad (6)$$

When the manipulated variable correction coefficient is introduced into the input voltage value of the operating interface, the corrected manipulated variable T_{xc} in the crosswise direction can be obtained by (7). Finally, the research flow of this study is shown in Fig. 12. The configuration of whole operation system is shown in Fig. 13.

$$T_{xc} = K_t T_x \quad (7)$$

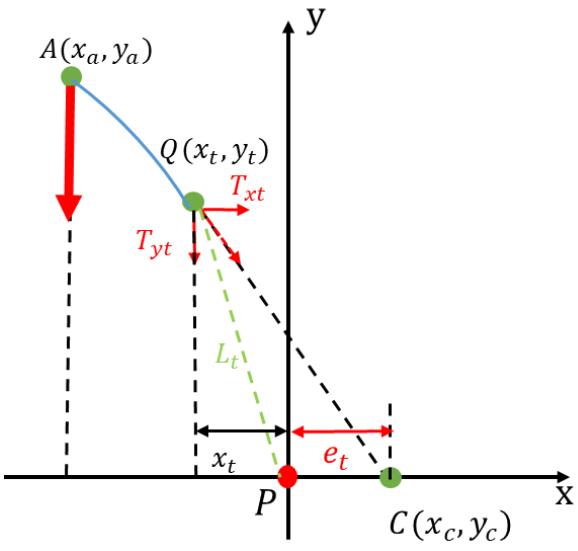

Fig. 11. Input voltage correction coefficient

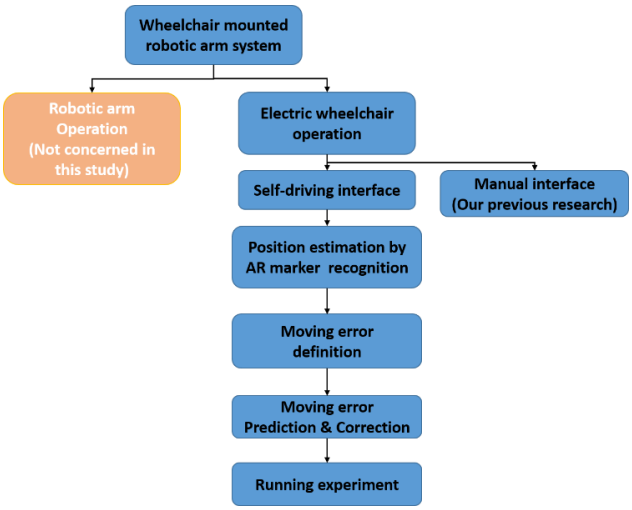

Fig. 12. Research flow of this study

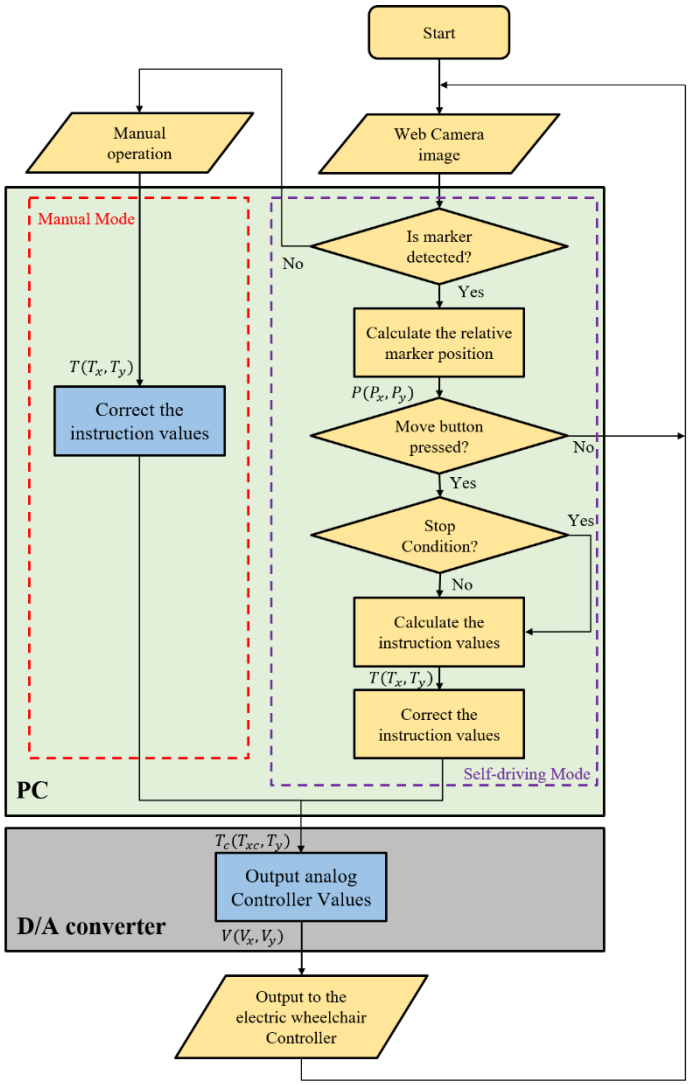

Fig. 13. Flowchart of the electric wheelchair operation system

V. EXPERIMENT

A. Self-driving Experiments

We conducted an experiment to verify the effectiveness of the proposed self-driving wheelchair operating system and error prediction/correction model by comparing the performance between the GUI with the proposed input voltage correction model and that without the model. To clearly recognize the AR marker, the upper limit of the distance between the wheelchair and the marker was set to 2.6 (m). Meanwhile, the camera is mounted to electric wheelchair and AR marker is set to the same height. The experimental subject is a healthy man. Experiments were carried out under the condition that the subject is sufficiently accustomed to the operation. As for the task of the experiment, we established three different running courses for the wheelchair as shown in Fig. 14.

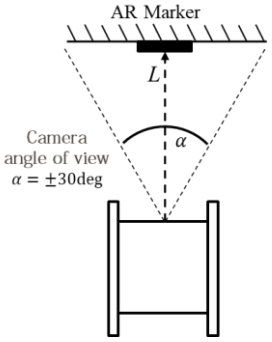

(a). Course A

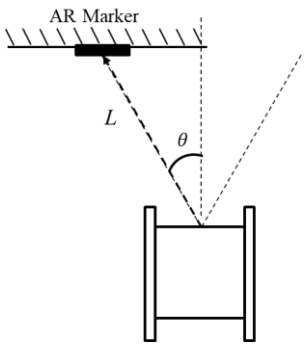

(b). Course B

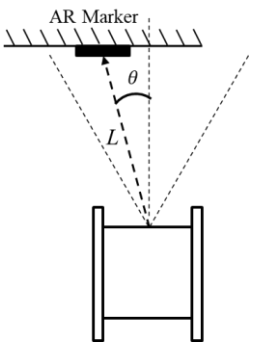

(c). Course C

Fig. 14. Running courses

The initial angle and the distance between the wheelchair and the AR marker for each course are shown in Table.1. In course A, the initial position of the wheelchair is directly in front of the AR marker, and the marker is projected in the center of the camera's visual field. In course B, the marker is projected at the edge of the field. In course C, the marker is projected infield at a certain angle. Finally, to evaluate the experiment we measured the velocity command voltage in the crosswise direction and the trajectory of the wheelchair.

Fig. 15 compares the velocity command voltage in the crosswise direction. In Fig. 15, the red curve represents the command voltage in the crosswise direction value of the system without the proposed correction model, and the blue curve represents the one with the correction model. The blue dashed line represents the neutral state of the wheelchair's command voltage.

TABLE I. INITIAL ANGLE AND DISTANCE IN COURSE A, B, AND C

	Initial angle θ (deg)	**Initial distance L (m)**
Course A	0.0	2.00
Course B	-25.0	2.15
Course C	-15.0	2.57

As a result, in course A, since the lateral distance is short, the change in the voltage command of the system with and without the correction model is not significant. The voltage command in both systems gradually converge on the neutral value and finally settled in the neutral value, which means the wheelchair complete the self-driving. In course B, it was first confirmed that, for a comparison with the original operating system, the system with the proposed correction model suppresses the command voltage in the crosswise direction significantly according to the predicted moving error, which reduce the moving speed in the crosswise direction and makes the target AR marker keep in the visual field of wheelchair mounted camera during the movement. In addition, in the case of the system without the correction model, since the marker disappears from the camera's visual field beginning at 3s, the command voltage stops updating and the wheelchair keeps going straight. In the case of the system with the correction model, it is also confirmed that the change in the command voltage in the corrected system is moderate, which means that the movement of the wheelchair in the lateral direction becomes smoother than that in the uncorrected system. The command voltage of the wheelchair finally reaches the neutral state (2.417v), which means that the wheelchair finally reaches the stop area. In course C, it is also confirmed that the command voltage is suppressed and that the change in the command voltage in the corrected system is moderate. Also, in case of the system with the correction model, converge on the neutral value and finally settled in the neutral value. On contrary, the command voltage in crosswise direction at the initial location is 1.75 times bigger for the system with the correction model than it is for the system without the correction model. The command voltage quickly approaches the neutral value once the moving started. However, the wheelchair's rapid speed causes an excessive amount of steering amplitude. In order to rectify the steering amplitude, at 1.3 seconds, the command voltage suppresses to a value lower than neutral, indicating that the wheelchair's motion direction switch is engaged., as shown in Fig. 15(c), but the marker disappears from the camera's visual field beginning at 2.5s finally.

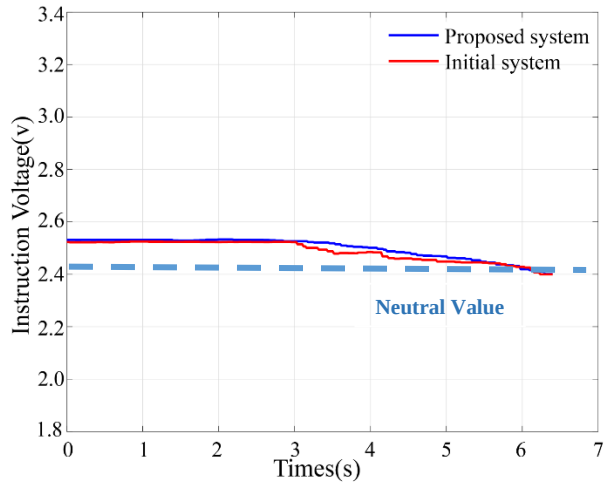

(a) Course A

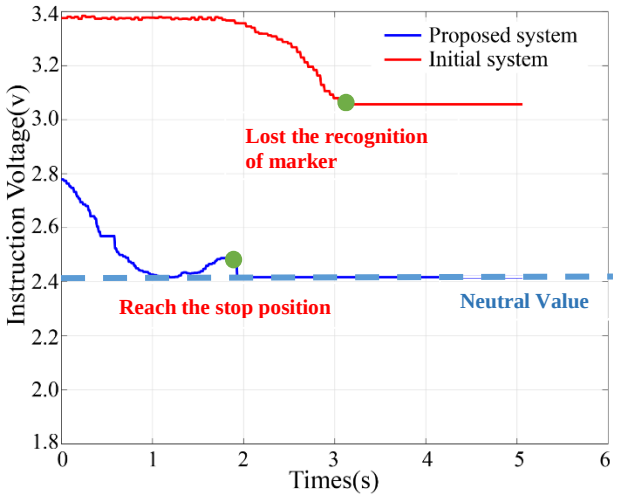

(b) Course B

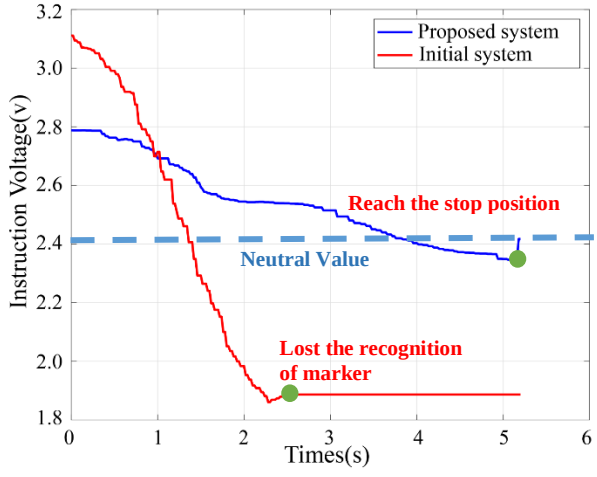

(c) Course C

Fig. 15. Comparison of the velocity command voltage

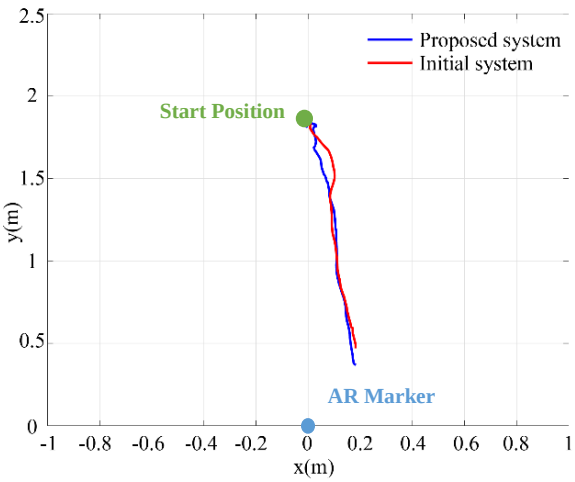

(a) Course A

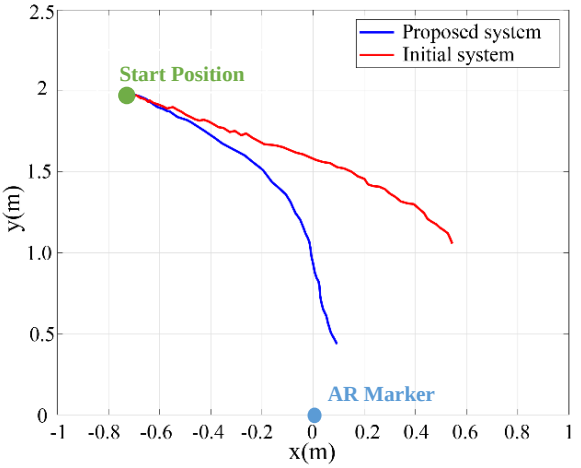

(b) Course B

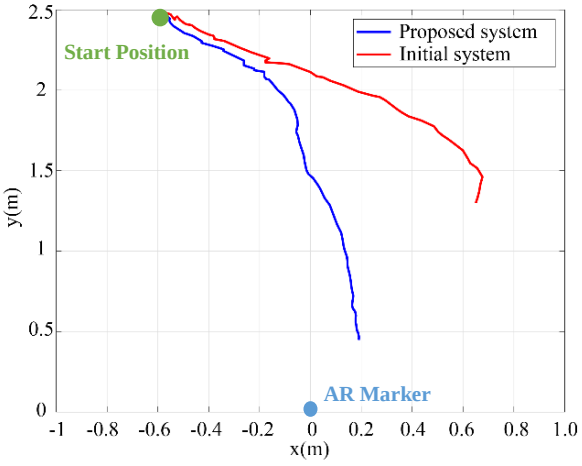

(c) Course C

Fig. 16. Comparison of the moving trajectory

Fig. 16 shows the moving trajectory of the wheelchair. The blue curve represents the wheelchair's moving trajectory in the case of the operating system with the proposed correction model, the red curve represents the uncorrected trajectory. Table 2 shows the stop position of the wheelchair and the calculated relative positions of the robotic arm and AR marker. In course A, when the initial position of the wheelchair is directly in front of the AR marker, the change in the trajectory with and without the correction is not significant because the distance in the lateral direction is short. In courses B and C, when the voltage correction coefficient is introduced, the wheelchair moves closer to the ideal trajectory than with the uncorrected system. In course B, within the uncorrected system, the AR marker disappears from the camera's visual field in the process of running, which makes it impossible for the wheelchair to reach the target position. In course C, although the wheelchair shows the tendency to correct the over steer, the AR marker still disappears from the camera's visual field, which shows the same result with Fig.15(c). In contrast, in the case of the operating system with the proposed correction model, the wheelchair reaches the target position and completes the self-drive.

TABLE II. RELATIVE POSITIONS OF ROBOTIC ARM AND AR MARKER

	Stop position of wheelchair(m)	**Relative position of AR marker(m)**
Course A	(0.368,0.000,0.183)	(0.368,0.230,0.033)
Course B	(0.450,0.000,0.157)	(0.450,0.230,0.007)
Course C	(0.467,0.000,0.190)	(0.467,0.230,0.040)

In comparison to the previous research [54], they proposed a self-driving system of wheelchair based on AR marker recognition. The position estimation system was conducted based on simplifying the wheelchair to a 2-wheeled model to make sure that the chair can complete the self-driving after the camera lost the sight of AR marker. However, in actual use, the movement of the caster also significantly affects the wheelchair, making realistic modeling of an electric wheelchair challenging. And the simplified wheelchair model may lead to an unavoidable accumulation of estimation error. On the other hand, in this research, we solve the same problem by collecting and analyzing the advance data of wheelchair movement, which avoids the wheelchair modelling. According to the experimental result, the proposed system modifying the trajectory of electric wheelchair and keeps the AR marker in the visual field during the hole running process, which fundamentally solved this problem.

B. Robotic Arm Simulation

We conducted a simulation experiment to verify whether the stop position of the wheelchair came within the working range of the robotic arm. The simulation environment was built by using Unity, a cross-platform game engine developed by Unity Technologies. In Fig. 17, the robotic arm is set to the initial posture with the end effector in the position of (0.28m, 0.4m, 0m) with the base of the arm being the origin, and the red cube indicates the target position. During the experiment, we calculated the relative positions of robotic arm and the target AR marker according to the wheelchair's stop position of courses A, B, and C. We then set these relative positions as the target positions to verify the movement of the arm. Fig. 18 shows the posture of the arm after reaching the target position. The red dashed line represents the arm's set working range. The left side shows the side view and the right side shows the top view of the final posture, respectively. Fig. 18 confirmed that in all courses, the wheelchair reached the arm's operating range.

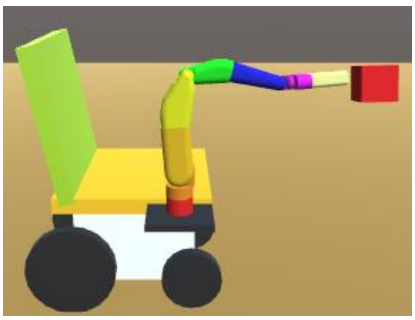

Fig. 17. Initial position of robotic arm in simulation

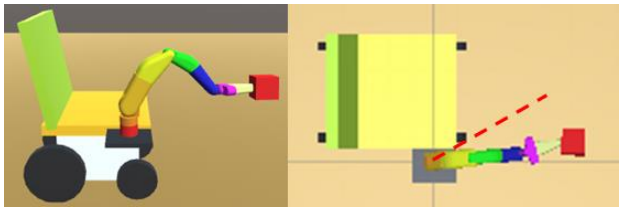

(a) Course A

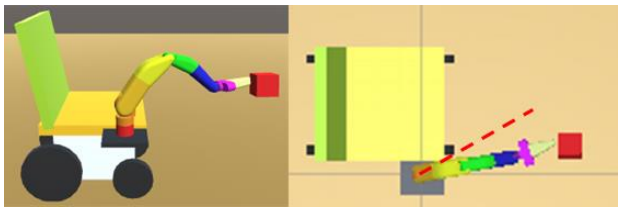

(b) Course B

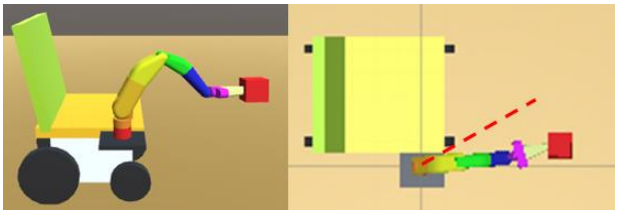

(c) Course C

Fig. 18. Final posture of the robotic arm or the stop position in each course

VI. CONCLUSION

In this study, we focus on the operation of an electric wheelchair in wheelchair-mounted robotic arm system and proposed a hybrid operating system for electric wheelchair that combines a manual-driving mode and a self-driving mode based on AR marker recognition. Meanwhile, to solve

the problem that the chair mounted camera lost the sight of the AR marker during self-driving, we also proposed an error prediction and correction model based on multiple linear regression analysis to modify the trajectory of wheelchair. In comparison to previous research, the proposed method avoids the complicated wheelchair modeling that is difficult to achieve in practice and solved the problem by data analyzing. Finally, we conducted a comparative experiment and a simulation experiment on three different running courses. By evaluating the command voltage and moving trajectory of the wheelchair, we showed the effectiveness of the proposed prediction and correction model. The robotic arm simulation showed that, in each running course, the wheelchair's stop position fit within the working range of the robotic arm.

As the future work, since we think the road condition also plays an important role in moving error, we intend to investigate how much this factor influences system accuracy. For the GUI, we planning to develop an operating system that integrates an electric wheelchair and a robotic arm and to verify the system's effectiveness by several operation tests.

REFERENCES

[1] Cabinet Office, "Annual Report on Government Measures for Persons with Disabilities," pp. 213, 2021, link: link: https://www8.cao.go.jp/shougai/whitepaper/index-w.htm .

[2] Cabinet Office, "Annual Report on Government Measures for Persons with Disabilities," pp. 1, 2011, link: link: https://www8.cao.go.jp/shougai/whitepaper/index-w.htm

[3] Y. Suga, W. Wang, S. Sugano, "Development of Light-Weight Robot Arm Mounted On Wheel Chair with Storage Mechanism," The Proceedings of JSME annual Conference on Robotics and Mechatronics (Robomec), 1A1-D14, 2010, doi: 10.1299 /jsmermd. 2010._1A1-A17_1.

[4] N. Yamanobe, Y. Wakita, "Daily Life Support for Persons with Upper-limb Disabilities by Robotic Arm," The 24th Annual Conference of the Japanese Society for Artificial Intelligence, 1H2-NFC3b-10, 2010, doi: 10.7210/jrsj.29.255 .

[5] V. Maheu, P. Archambault, J. Frappier, F. Routhier, "Evaluation of the JACO robotic arm: Clinico-economic study for powered wheelchair users with upper-extremity disabilities," IEEE International Conference on Rehabilitation Robotics, pp. 1-5, 2011, doi: 10.1109/ICORR.2011.5975397.

[6] J. Vogel, D. Leidner, A. Hagengruber, M. Panzirsch, B. Bauml, M. Denninger, U. Hillenbrand, L. Suchenwirth, P. Schmaus, M. Sewtz, A. Bauer, T. Hulin, M. Iskandar, G. Quere, A. Albu-Schaffer, A. Dietrich, "An Ecosystem for Heterogeneous Robotic Assistants in Caregiving: Core Functionalities and Use Cases," IEEE Robotics & Automation Magazine, vol. 28, no. 3, pp. 12-28, 2021, doi: 10.1109/MRA.2020.3032142.

[7] W. Yoon, Y. Wakita, N. Yamanobe, "Self-reliance Support by RAPUDA, a Robot Arm that Supports the Lives of People with Disabilities in the Upper Limbs," Journal of the Society of Biomechanisms, vol. 37, no. 2, pp. 100-104, 2013, doi: 10.3951/sobim.37.100.

[8] C. Chung, H. Ka, H. Wang, D. Ding, A. Kelleher, A. Cooper, "Performance Evaluation of a Mobile Touchscreen Interface for Assistive Robotic Manipulators: A Pilot Study," Top Spinal Cord Inj Rehabil, vol. 23, no. 2, pp. 131–139, 2017, doi: 10.1310/sci2302-131.

[9] K. Ichikawa, T. Oka, K. Matsusima, "The Evaluation of Manipulator Operation Interface Using 3D Mouse," The 78th National Convention of IPSJ, 2Y-01, 2016.

[10] K. Sudheer, T. V. Janardhana Rao, C. Sridevi, M. S. MadhanMohan, "Voice and Gesture Based Electric-Powered Wheelchair Using Arm," International Journal of Research in Computer and Communication technology (IJRCCT), vol. 1, no. 6, pp. 278-283, 2012.

[11] K. Yamasaki, M. Anraku, T. Shibata, M. Suwa, "Electric Wheelchair Control Using Head Velocity-Based Gesture Recognition Specializing in Turning Motion," Proceeding of LEM21, pp. 646-650, 2021, doi: 10.1299 /jsmelem. 2021.10.125-118.

[12] M. Mazo, F. J. Rodríguez, J. L. Lazaro, J. Urena, J. C. García, E. Santiso, P. A. Revenga, "Electronic control of a wheelchair guided by voice commands," Control Engineer Practice, vol. 3, no. 5, pp. 665-674, 1995, doi: 10.1016/0967-0661(95)00042-S.

[13] H. Jiang, T. Zhang, J. Wachs, Bradley Duerstock, "Enhanced Control of a Wheelchair-mounted Robotic Manipulator Using 3D Vision and Multimodal Interaction," Computer Vision and Image Understanding, vol. 149, pp. 21-31, 2016, doi: 10.1016/j.cviu.2016.03.015.

[14] D. Wang, H. Yu, "Development of the control system of a voice-operated wheelchair with multi-posture characteristics," 2017 2nd Asia-Pacific Conference on Intelligent Robot Systems, pp. 151-155, 2017, doi: 10.1109/ACIRS.2017.7986083.

[15] R. Alonso, E. Concas, "An Abstraction Layer Exploiting Voice Assistant Technologies for Effective Human—Robot Interaction," Applied Sciences, vol. 11, no. 19, p. 9165, 2021, doi: 10.3390/app11199165.

[16] K. Lee, W. Chang, S. Kim, C. Im, "Real-Time "Eye-Writing" Recongition Using Electrooculogram (EOG)," IEEE Transactions on Neural Systems and Rehabilitation Engineering, vol. 25, no. 1, pp. 37-48, 2016, doi: 10.1109/TNSRE.2016.2542524.

[17] C. Ishii, "Control of an Electric Wheelchair Based on EMG, EOG and EEG," Journal of the Japan Society for Precision Engineering, vol. 83, pp. 1006–1009, 2017, doi: 10.2493/jjspe.83.1006.

[18] J. Lopes, M. Simao, N. Mendes, M. Safeea, J. Afonso, P. Neto, "Hand/arm Gesture Segmentation by Motion Using IMU and EMG Sensing," 27th International Conference on Flexible Automation and Intelligent Manufacturing, pp. 107-113, 2017, doi: 10.1016/j.promfg.2017.07.158.

[19] C. Han, Y. Kim, D. Kim, S. Kim, Z. Nenadic, C. Im, "Electroencephalography-based endogenous brain-computer interface for online communication with a completely locked-in patient," Journal of Neuro Engineering and Rehabilitation, vol. 16, no. 18, 2019, doi: 10.1186/s12984-019-0493-0.

[20] W. Chen, S. Chen, Y. Liu,Y. Chen, C. Chen, An Electric Wheelchair Manipulating System Using SSVEP-Based BCI System," Biosensors, vol. 12, no. 10, p. 772, 2022, doi: doi.org/10.3390/bios12100772.

[21] M. Paing, A. Juhong, C. Pintavirooj, "Design and Development of an Assistive System Based on Eye Tracking," Electronics, vol. 11, no. 4, p. 535, 2022, doi: 10.3390/electronics11040535.

[22] N. Siribunyaphat, Y. Punsawad, "Steady-State Visual Evoked Potential-Based Brain–Computer Interface Using a Novel Visual Stimulus with Quick Response (QR) Code Pattern," Sensors, vol. 22, no. 4, p. 1439, 2022, doi: 10.3390/s22041439.

[23] L. Yang, T. Ichikawa,Y. Miyawaki, R. Sakamoto, N. Kato, K.Yano, S. Shimada, "Maloperation Prevention Filter for Touchscreen Used in Robot Arm," Journal of Physics: Conference Series, vol. 1267, pp. 1–6, 2019, doi: 10.1088/1742-6596/1267/1/012075.

[24] P. Abolghasemi, R. Rahmatizadeh, A. Behal, L. Boloni, "A Real-Time Technique for Positioning a Wheelchair-Mounted Robotic Arm for Household Manipulation Tasks," The Workshop Program of the Association for the Advancement of Artificial Intelligence's Thirtieth AAAI Conference on Artificial Intelligence, WS-16-01, pp. 2-7, 2016.

[25] J. Wang, T. Wang, C. Yao, X. Li, C. Wu, "Active Tension Control for WT Wheelchair Robot by Using a Novel Control Law for Holonomic or Nonholonomic Systems," Mathematical Problems in Engineerning, vol. 2014, 2014, doi: 10.1007/s11432-014-5142-4.

[26] National Rehabilitation Center for Persons with Disabilities, "Electric Wheelchair Compatibility & Operation Practice Manual," pp.8, 2006, link: https://iss.ndl.go.jp/books/R100000002-I000010852516-00.

[27] A. Ma'arif, A. A. Nuryono, and Iswanto, "Vision-Based Line Following Robot in Webots," 2020 FORTEI-International Conference on Electrical Engineering (FORTEI-ICEE), 2020, pp. 24-28, doi: 10.1109/FORTEI-ICEE50915.2020.9249943.

[28] A. Boubakri, S. Mettali Gamar, "A New Architecture of Autonomous Vehicles: Redundant Architecture to Improve Operational Safety," International Journal of Robotics and Control Systems, vol. 1, no. 3, pp. 355-368, 2021, doi: 10.31763/ijrcs.v1i3.437.

[29] A. N. Ouda, Amr Mohamed, "Autonomous Fuzzy Heading Controlfor a Multi-Wheeled Combat Vehicle," International Journal of Robotics and Control Systems, vol. 1, no. 1, pp. 90-101, 2021, doi: 10.31763/ijrcs.v1i3.380ijrcs.

[30] S. Bach, S. Yi, "An Efficient Approach for Line-Following Automated Guided Vehicles Based on Fuzzy Inference Mechanism," Journal of Robotics and Control, vol. 3, no. 4, 2022, doi: 10.18196/jrc.v3i4.14787.

[31] Y. Yasumuro, S. Kusakabe, H. Dan, "3D Barrier-Free Verification for Wheelchair Accsee," Proceedings of the 13th International Conference on Construction Applications of Virtual Reality, pp. 564-571, 2013.

[32] K. Tobita, Y. Shikanai, K. Mima, "Study on Automatic Operation of ManualWheelchair Prototype and Basic Experiments," Journal of Robotics and Mechatronics, vol. 33, no. 1, pp. 69-77, 2021, doi: 10.20965/jrm.2021.p0069.

[33] M. A. Shamseldin, E. Khaled, A. Youssef, D. Mohamed, S. Ahmed, "A New Design Identification and Control Based on GA Optimization for an Autonomous Wheelchair," Robotics, vol. 11, no. 5, 2022, doi: 10.3390/robotics11050101.

[34] B. Ngo and T. Nguyen, "A Semi-Automatic Wheelchair with Navigation Based on Virtual-Real 2D Grid Maps and EEG Signals," Applied Science, vol. 12, no. 17, 2022, doi: 10.3390/app12178880.

[35] S. Thrun, W. Burgard, and D. Fox, "Probabilistic Robotics," The MIT Press, 2005.

[36] Y. Mori, K. Nagao, "Automatic Generation of Multidestination Routesfor Autonomous Wheelchairs," Journal of Robotics and Mechatronic, vol. 32, no. 6, pp. 1121-1136, 2020, doi: 10.20965/jrm.2020.p1121.

[37] C. Gao, M. Sands, J. Spletzer, "Towards Autonomous Wheelchair Systems in Urban Environments," Springer Tracts in Advanced Robotics, vol. 62, pp. 13–23, 2010, doi: 10.1007/978-3-642-13408-1_2.

[38] H. Grewal, A. Matthews, R. Tea, K. George, LIDAR-based autonomous wheelchair, 2017 IEEE Sensors Applications Symposium, 2017, doi: 10.1109/SAS.2017.7894082.

[39] M. Yokozuka, O. Matsumoto, "Accurate Localization for Making Maps to Mobile Robots Using Odometry and GPS Without Scan-Matching," Journal of Robotics and Mechatronics, vol. 27, no. 4, pp. 410-418, 2015, doi: 10.20965/jrm.2015.p0410.

[40] W. Rahiman, Z. Zainal, "An Overview of Development GPS Navigation for Autonomous car," IEEE 8th Conference on Industrial Electronics and Applications, pp. 1112-1118, 2013, doi: 10.1109/ICIEA.2013.6566533.

[41] N. Aktar, I. Jaharr, B. Lala, "Voice Recognition based intelligent Wheelchair and GPS Tracking System," 2019 International Conference on Electrical, Computer and Communication Engineering, pp. 1-5, 2019, doi: 10.1109/ECACE.2019.8679163.

[42] C. Qinghua, Z. Taihu., X. Yihong, S. Hongyu, "Design and Realization of Intelligent Wheelchair Based on STM32," Journal of Physics: Conference Series, vol. 1678, p. 012114, 2020, doi: 10.1088/1742-6596/1678/1/012114.

[43] N. Yokoya, "Mixed Reality: Merging Real and Virtual Worlds: I Introduction," Systems, Control And Information, vol. 49, no. 12, pp. 489-494, 2005, doi: 10.11509/isciesci.49.12_489.

[44] S. Hashizume, I. Suzuki, K. Takazawa, R. Sasaki, Y. Ochiai, "Telewheelchair: the Remote Controllable Electric Wheelchair System combined Human and Machine Intelligence," Proceedings of the 9th Augmented Human International Conference, pp. 1-9, 2018, doi: 10.1145/3174910.3174914.

[45] M. Zolotas, J. Elsdon, and Y. Demiris, "Head-mounted augmented reality for explainable robotic wheelchair assistance," 2018 IEEE/RSJ International Conference on Intelligent Robots and Systems, 2018, doi: 10.1109/IROS.2018.8594002.

[46] K. Motooka, T. Okawara, K. Go, Y. Yamato, A. Miyata, "Study on Distance Reduction of a Barrier Simulator Using an HMD and an Electric Wheelchair," The 24th Annual Conference of the Virtual Reality Society of Japan, 2019.

[47] R. Quesada, Y. Demiris, "Augmented Reality Controlled Smart Wheelchair Using Dynamic Signifiers for Affordance Representation," IEEE/RSJ International Conference on Intelligent Robots and Systems, pp 4812-4818, 2019, doi: 10.1109/IROS40897.2019.8968290.

[48] N. Matsunaga, Y. Takeuchi, H. Okajima, "A Construction Method of Obstacle Avoidance System for Welfare Vehicle by Spatial Mapping of Driving Environment using Mixed Reality," Transactions of the JSME, vol. 87, no. 894, pp. 1-16, 2021, doi: 10.1299/transjsme.20-00033.

[49] T. Mizunami, Y. Sakamura, A. Tomita, K. Inoue, I. Kitahara, E. Harada, "Reduction of Anxiety for an Autonomous Vehicle by Augmented Visual Information," The 82nd Annual Convention of the Japanese Psychological Association, 3EV-056, 2018 doi: 10.4992/pacjpa.82.0_3EV-056 .

[50] H. Otsuka, R. Yajima, K. Nagatati, D. Kubo, "Localization of a Small Multi−rotor UAV Using Dropping AR Markers," The Proceedings of JSME annual Conference on Robotics and Mechatronics, 2A2-G02, 2015, doi: 10.1299/jsmermd.2015._2A2-G02_1.

[51] F. Sato, T. Koshizen, T. Matsumoto, H. Kawase, S. Miyamoto, Y. Torimoto, "Self-driving system for electric wheelchair using smartphone to estimate travelable areas," 2018 IEEE International Conference on Systems, Man, and Cybernetics, pp. 298–304, 2018, doi: 10.1109/SMC.2018.00061.

[52] J. Yu,W. Jiang, Z. Luo, and L. Yang, "Application of a Vision-Based Single Target on Robot Positioning System," Sensors, vol. 21, no. 5, p. 1829, 2021, doi: 10.3390/s21051829.

[53] M. Teoh,K. Teo, H. Yoong, "Numerical Computation-Based Position Estimation for QR Code Object Marker: Mathematical Model and Simulation," Computation, vol. 10, no. 9, p. 147, 2022, doi: 10.3390/computation10090147.

[54] J. Kato, G. Deguchi, J. Inoue, M. Iwase, "Improvement of Performance of Navigation System for Supporting Independence Rehabilitation of Wheelchair – Bed Transfer," Journal of Physics: Conf. Series, vol. 1487, p. 012041, 2020, doi: 10.1088/1742-6596/1487/1/012041.

[55] P. Hebert, J. Ma, J.Borders, A.Aydemir, M. Bajracharya, N. Hudson, K. Shankar, S. Karumanchi, B. Douillard, J. Burdick, "Supervised Remote Robot with Guided Autonomy and Teleoperation (SURROGATE): A Framework for Whole-Body Manipulation," IEEE International Conference on Robotics and Automation, pp. 5509-5516, 2015, doi; 10.1109/ICRA.2015.7139969.

[56] L. Yang, T .Ichikawa, R. Sakamoto, T. Itami, N. Kato, K. Yano, S. Shimada, "Robot Arm Operating Interface Using a Touch Panel for Gripping an Object on the Floor by Designating the End Effector," 2020 IEEE/SICE International Symposium on System Integration, pp. 401–404, 2020, doi: 10.1109/SII46433.2020.9026233 .

[57] E. Tanaka, T. Ichikawa, R. Sakamoto, K. Yano, S. Shimada, "7-DOF Robot Arm "Udero" for Self-Reliance Support of Disabled Persons," The 17th SICE System Integration Division Annual Conference, 2016.

[58] Y. Miyawaki, L. Yang, R. Sakamoto, N. Kato, K. Yano, S. Shimada, "Interface for Operating Electric Wheelchair without Gazing Operation Screen," JSME The Proceedings of Conference of Tokai Branch, vol. 68, 2019, doi: 10.1299/jsmetokai.2019.68.519.

[59] Y. Miyawaki, L. Yang, R. Sakamoto, N. Kato, K. Yano, P. Minyong, "Electric Wheelchair Control System without Gazing the Operation Screen," The 9th TSME International Conference on Mechanical Engineering, p. 2017-0105, 2018.

[60] H. Kato, "ARToolKit: Library for Vision-based Augmented Reality," IEICE Technical Report, vol. 101, no. 652, pp.79–86, 2002.

[61] H. Tanaka, K. Ogata, Y. Matsumoto, "Improving the accuracy of visual markers by four dots and Image interpolation," 2016 International Symposium on Robotics and Intelligent Sensors, pp. 178–183, 2016, doi: 10.1109/IRIS.2016.8066087.

[62] F. Sato, "Improvement of Self Position Estimation of Electric Wheelchair Combining Multiple Positioning Methods," Advanced Information Networking and Applications, pp 607–618, 2019, doi: 10.1007/978-3-030-15032-7_51.